Received: 21 January 2024 | Accepted: 12 July 2024

DOI: 10.1111/1462-2920.16686

BRIEF REPORT

ENVIRONMENTAL MICROBIOLOGY

Transient, context-dependent fitness costs accompanying viral resistance in isolates of the marine microalga *Micromonas* sp. (class Mamiellophyceae)

Anamica Bedi de Silva[1] | **Shawn W. Polson**[2] | **Christopher R. Schvarcz**[1] | **Grieg F. Steward**[1] | **Kyle F. Edwards**[1]

[1]Department of Oceanography, University of Hawai'i at Mānoa, Honolulu, Hawaii, USA

[2]Center for Bioinformatics and Computational Biology & Department of Computer and Information Sciences, University of Delaware, Newark, Delaware, USA

Correspondence
Kyle F. Edwards, Department of Oceanography, University of Hawai'i at Mānoa, Honolulu, HI 96822, USA.
Email: kfe@hawaii.edu

Funding information
Simons Foundation; National Science Foundation, Grant/Award Numbers: OCE 1559356, OCW 2129697, RII Track-2 FEC 1736030

Abstract

Marine microbes are important in biogeochemical cycling, but the nature and magnitude of their contributions are influenced by their associated viruses. In the presence of a lytic virus, cells that have evolved resistance to infection have an obvious fitness advantage over relatives that remain susceptible. However, susceptible cells remain extant in the wild, implying that the evolution of a fitness advantage in one dimension (virus resistance) must be accompanied by a fitness cost in another dimension. Identifying costs of resistance is challenging because fitness is context-dependent. We examined the context dependence of fitness costs in isolates of the picophytoplankton genus *Micromonas* and their co-occurring dsDNA viruses using experimental evolution. After generating 88 resistant lineages from two ancestral *Micromonas* strains, each challenged with one of four distinct viral strains, we found resistance led to a 46% decrease in mean growth rate under high irradiance and a 19% decrease under low. After a year in culture, the experimentally selected lines remained resistant, but fitness costs had attenuated. Our results suggest that the cost of resistance in *Micromonas* is dependent on environmental conditions and the duration of population adaptation, illustrating the dynamic nature of fitness costs of viral resistance among marine protists.

INTRODUCTION

Marine viruses influence oceanic biogeochemical processes through the infection of single-celled organisms such as bacteria, archaea, and protists (Fuhrman, 1999; Suttle, 2007). An important aspect of microbe-virus interactions is the ability of microbes to evolve defences against viral infection (Breitbart, 2012). Although resistance to infection is commonplace among marine microbes in both laboratory and field settings (Thyrhaug et al., 2003; Waterbury & Valois, 1993), the persistence of susceptible hosts suggests a fitness cost associated with viral protections (Lennon et al., 2007; Lenski, 1988). The fitness costs of resistance to infections by lytic viruses are likely to have broad consequences for ecosystems, such as altering the growth rate and productivity of microbial communities, and influencing the portion of microbial production that is lysed rather than consumed by predators (Våge et al., 2013).

Much of the early work investigating the evolutionary responses of microscopic marine plankton to viral infections focused on bacteria (see Breitbart, 2012 and references therein), but there is growing interest in how selection by viruses might influence the phenotype of unicellular eukaryotes.

A common metric of fitness is growth rate, which has been observed to decrease in some resistant strains of prokaryotes (Lennon et al., 2007). In eukaryotic algae, Frickel et al., 2016 found a negative correlation between breadth of resistance and growth rate in the freshwater alga *Chlorella variabilis*, using host strains that co-evolved with viruses in a long-term chemostat experiment. In another study, resistant morphotypes of *Emiliania huxleyi*

showed a 15%–55% decrease in growth rate compared to ancestral strains (Frada et al., 2017). However, virus resistance was not accompanied by a detectable decline in growth rate in several other studies with various eukaryotic phytoplankton such as *E. huxleyi*, *Ostreococcus tauri*, and *Micromonas* sp. (Ruiz, Baudoux, et al., 2017; Ruiz, Oosterhof, et al., 2017; Thomas et al., 2011).

Quantifying a cost of resistance (COR) is challenging in part because the nature and magnitude of fitness costs may vary with context, such as the physiological condition of the host, and may also depend on the (co) evolutionary history of the host and virus populations. Bohannan et al. (1999) found that fitness costs for *Escherichia coli* varied depending on the phage strain to which cells were resistant and whether resistant cells were grown in a glucose-, trehalose-, or maltose-limiting medium. Previous studies on phytoplankton did not find an effect of resource levels on fitness costs (Heath et al., 2017; Lennon et al., 2007), but it is possible that shifts in COR would emerge under a different, or more severe, resource limitation. Furthermore, the magnitude of fitness costs could be affected by the coevolutionary history of hosts and viruses. Past experiments to measure fitness costs have used host strains and viruses that were isolated from different water masses and/or kept separately in culture for years at a time (Heath et al., 2017; Ruiz, Baudoux, et al., 2017; Ruiz, Oosterhof, et al., 2017). It is possible that hosts and viruses with recent coevolutionary interactions will exhibit a different COR if a virus is better adapted to its host and/or if a coevolutionary arms race has enhanced mutual adaptation (see Schwartz & Lindell, 2017; Thyrhaug et al., 2003). While not specifically examining geography or habitat of cells and viruses, Lennon et al. (2007) did provide evidence that the magnitude of the reduction in growth rates among resistant *Synechococcus* varied according to the identity of ancestral strains, indicating that the genetic background of a host may influence the cost of adapting to a particular virus.

Another consideration when trying to make sense of coevolutionary dynamics is that the time since acquiring resistance appears to affect the presence of COR. Avrani & Lindell, 2015 found that COR attenuated over time in seven strains of the prokaryote *Prochlorococcus* using experimentally selected cultures that were subsequently propagated for 40 months. The authors identified both new genetic mutations and reversions that may have compensated for the initial decline in growth rate.

To better understand the ecological and evolutionary dynamics of eukaryotes and eukaryotic viruses, we used two isolates of the ubiquitous marine eukaryotic alga *Micromonas* and four dsDNA-containing viruses in the genus *Prasinovirus* that were co-isolated from the same coastal waters of Kāneʻohe Bay, Hawaiʻi. *Micromonas* is a ~2 μm diameter flagellated prasinophyte found in all major ocean basins (Cottrell & Suttle, 1995; Demory et al., 2018; Thomsen & Buck, 1998). Previously isolated *Micromonas* dsDNA viruses are lytic viruses (capsid size ca. 100 nm) in the family *Phycodnaviridae* similarly found in all ocean basins (Bellec et al., 2009; Cottrell & Suttle, 1991; Waters & Chan, 1983; Wilson et al., 2009; Zingone, 1999). Using our Kāneʻohe Bay isolates we conducted experimental evolution to generate resistant algal strains, which allowed us to focus on trait changes caused by resistance, controlling for other processes that could influence trait variation. Growth assays under different light conditions were used to test the interactive effects of resistance and resource limitation on fitness.

EXPERIMENTAL PROCEDURES

Micromonas and MicV isolates

The UHM phytoplankton collection contains seven *Micromonas* sp. strains. Six of these, including the two used to generate cell lines in this study, were isolated by Schvarcz (2018) from the surface waters (>2 m) of Kāneʻohe Bay, Oʻahu, Hawaiʻi (21°27 N, 157°48 W) in 2011. Additionally, a *Micromonas* sp. strain was isolated from surface waters (< 25 m) at the oligotrophic site Station ALOHA, ~100 km north of Oʼahu (22°45 N, 158°00 W) in 2012. A dsDNA virus strain was isolated on each one of the seven *Micromonas* sp. strains using water from the same location of each host, in 2011 for Kāneʻohe virus strains and in 2015 for the Station ALOHA virus strain. Full descriptions of cell and virus strains can be found in Schvarcz (2018). Each of the seven cell lines exhibits different cross-infection dynamics when challenged separately with the seven virus strains. Two *Micromonas* strains were chosen for this study out of the seven strains in our collection, given their amenability to culturing and susceptibility to multiple isolated virus strains (each susceptible to 3 of the 7 virus strains in our collection), which allowed for the selection of resistance against multiple virus strains (Figure S1). These two *Micromonas* sp. strains were isolated from Kāneʻohe Bay with original isolate identifiers of KB-FL13 and KB-FL42 (Schvarcz, 2018) and were assigned the University of Hawaiʻi at Mānoa (UHM) culture collection identifiers of UHM1061 and UHM1065. For simplicity, in the presentation of this paper, these cell lines are referred to as M1 and M2, respectively. The *Micromonas* cell line originating from Station ALOHA, UHM1080 (referred to as AL-FL30 in Schvarcz, 2018), was not included in phenotypic assay but was included in phylogenetic analysis described below.

Cell cultures were maintained in *f*/2-Si medium (Guillard, 1975; Guillard & Ryther, 1962) at 25°C with an irradiance of ~100 μE m^{-2} s^{-1} provided by Philips

F17T8/TL841 17-W fluorescent bulbs. The irradiance level of 100 μE m^{-2} s^{-1} is typically near the optimum for growth of marine phytoplankton (Edwards et al., 2015). Cultures were transferred approximately every 2 weeks by diluting to 1% in fresh medium. Four viruses with the UHM culture collection IDs McV-KB1, McV-KB2, McV-KB3, and McV-KB4, (corresponding to viruses isolated on hosts KB-FL13, KB-FL22, KB-FL28, and KB-FL42 in Schvarcz, 2018) were used in the selection process for resistant hosts. For simplicity of presentation, McV-KB1, McV-KB2, McV-KB3, and McV-KB4 will be referred to here as V1, V2, V3, and V4, respectively. The gene sequences of a fifth virus, MsV-SA1, isolated from waters of Station ALOHA on the cell line UHM1080, was used in phylogenetic analysis. Viral stocks were maintained by challenging exponentially growing cultures of respective isolated host strains approximately every 2 weeks. Lysates were filtered with a 0.2 μm syringe filter once algal cultures were visually cleared. The resulting filtrate was then stored at ~4°C.

Phylogenetic analysis of host and virus isolates

Gene phylogenies were constructed using the 18S rRNA gene for *Micromonas* isolates, and the DNA polymerase gene Beta (*polB*) for the viruses. Genomes of M1 and M2 were sequenced with PacBio Sequel II technology at the University of Delaware DNA Sequencing and Genotyping Center. Genome assembly of cellular DNA was conducted at the University of Delaware Bioinformatics Data Science Core using Canu ver 1.9 (Koren et al., 2017) and 18S rRNA gene sequences were identified in genome assemblies using the Basic Local Alignment Search Tool (Altschul et al., 1990) against *Micromonas* sp. RCC299's 18S rRNA partial gene sequence (HM191693).

Phylogenetic analysis of M1 and M2 18S rRNA genes was carried out using closely related sequences found via nucleotide BLAST against GenBank (Sayers et al., 2022). Using Geneious 11.1.5, full and near-full gene sequences were aligned. The resulting 1771 bp alignment was used to generate a phylogenetic tree using FastTree 2.1.12 (Price et al., 2010) in Geneious using default settings.

The genomes of the four viruses were sequenced with Illumina paired-end 151 bp technology at the Microbial Genomic Sequencing Center at the University of Pittsburgh. Partial de novo assemblies were created in Geneious 11.1.5. A phylogenetic tree was constructed for the B-family DNA polymerase (*polB*) gene, which is commonly used as marker gene for *Phycodnaviridae* (Chen & Suttle, 1995). The *polB* genes in our sequences were identified by BLAST search using published *Micromonas* virus sequences as the query. Differences in base-call quality among reads for the putative *polB* gene of V1 indicated the presence of two strains. The contig containing the *polB* sequence was dissolved and re-assembled with high stringency to resolve contaminating sequences. To construct a phylogeny, *polB* sequences similar to each of our four viruses were found through a BLASTn search against the NCBI nucleotide database. We included 108 published *polB* sequences, as well as a *polB* sequence from a virus isolated on UHM1080, to create a 453 bp alignment using MAFFT accessed through Geneious. FastTree was then used to construct a phylogeny in Geneious using default settings.

Establishing susceptible and resistant host strains

We were unable to grow *Micromonas* on solid media and used dilution-to-extinction procedure in liquid medium to isolate resistant cell lines. The ancestral M1 and M2 cultures are highly susceptible to lysis but may contain a low frequency of resistance mutants. To isolate strains grown from single resistant cells, 3.5 mL susceptible M1 and M2 cultures with cell density of 10^6 cells/mL were serially diluted 10-, 10^2-, and 10^3-fold. For each dilution, 2 mL aliquots were transferred to all the wells of a 24-well untreated CELLSTAR® suspension culture plate and then challenged during exponential growth with 500 μL fresh, undiluted, viral lysate (~10^7 infectious particles/mL). We combined dilution and viral inoculation to increase the probability that each resistant line would be derived from a single cell and that different resistant lines would potentially represent different genotypes. Given that the highest dilution in our series was 10^3, and our lysate had 10^7 infectious particles/mL, the lowest concentration of infection particles was 10^4 infectious particles/mL. As our host organisms are motile flagellates, encounter rates of cells and viruses would provide sufficient viral pressure.

Plates were incubated (25°C, ~100 μE m^{-2} s^{-1}, 12:12 light: dark cycle) and routinely examined at 400× with an inverted microscope until resistant mutants grew to a density detectable by microscopy (≥ 10^3 cells mL^{-1}), taking approximately 3–4 weeks. Approximately 10% of wells from the highest dilution plate of each host-virus strain combination contained detectable cells, which were used to establish new 3.5 mL cultures. Once in exponential growth, the putative resistant lines were re-challenged with viral lysate and monitored for signs of lysis to verify resistance. Susceptible ancestors were put through the same dilution and pipetting steps, without the addition of lysate, in order to control for phenotypic evolution arising from the genetic bottlenecks and selection associated with these steps. As with the resistant strains, cells growing back at the highest dilution were used to establish

TABLE 1 Number of resistant and susceptible host cell lines (M) isolated after inoculation with different viruses (V).

M1 descendants	*M1S*	*M1V1*	*M1V2*	*M1V3*	
# of isolates	23	11	23	10	
M2 descendants	***M2S***		***M2V2***	***M2V3***	***M2V4***
# of isolates	24		13	18	13

Note: Susceptible isolates are indicated by the letter 'S' at the end of the strain name. Grey cells indicate a host-virus cross that did not result in lytic infection.

experimental cultures. The resulting susceptible strains were named by appending 'S' to the ancestral host code name. Multiple strains (from 10 to 24) of each susceptible or resistant strain type were generated (Table 1).

Thomas et al., 2011 reported viral budding in cultures of *O. tauri* that had been selected for resistance, suggesting that a shift from lytic to chronic infection could underlie the resistant phenotype. To confirm that resistant lines in our experiment were truly resistant and not under chronic infection, resistant cell cultures were filtered (0.2 μm) and the resulting filtrate was added to susceptible host cultures. These cultures were then monitored for reductions in cell density over the course of 2 weeks.

High and low light growth experiment

Growth experiments were conducted over 3–4 weeks, during which 135 cell lines (Table 1) were grown in untreated 24-well CELLSTAR® suspension plates (2.5 mL culture volume). All descendant cell lines were grown in both low light (~10 μE m^{-2} s^{-1}) and high light (~100 μE m^{-2} s^{-1}), with duplicates of every line in each light condition. Each resistance assay included susceptible ancestors as a positive control, both to confirm viral lytic activity and to serve as a point of reference for population decline. All cultures were grown in the same Percival AL36L4 growth chamber with cool white lights mounted above individual shelves adjusted to either high or low light conditions.

Daily growth data was collected for each well via fluorescence readings in a plate reader (TECAN Spark). Preliminary experiments found that fluorescence values correlate strongly with haemocytometer-based cell counts of *Micromonas*. Cultures were transferred into a new plate with fresh medium on a semi-weekly basis to maintain exponential phase growth. Cultures were acclimated to experimental conditions before measuring growth rates. The duration required for acclimation was one transfer under high light (i.e., one round of growth from inoculation to stationary phase), and two transfers under low light.

Maintaining cultures in exponential growth throughout the experiment allowed us to generate multiple exponential growth curves for each cell line. We obtained approximately 520 growth curves which were used to estimate the growth rates for each experimental isolate. A linear regression was fit to exponential phase data using R software in order to extract exponential growth rates (R Core Team, 2022). We used a mixed model to determine if growth rates were affected by susceptibility (resistant vs. susceptible) and light level (high vs. low) for each experimental sample with R package glmmTMB (Brooks et al., 2012) using the following terms:

$$growth\ \ rate \sim susceptibility + light + susceptibility{:}light + (1|plate) + (1|isolate)$$

where *growth rate* (the response variable) is modelled as a function of the terms to the right of the '~' (the predictor variables). Here, '*susceptibility*:*light*' is an interaction term that accounts for any interactive effects of light and susceptibility. The terms (1|plate) and (1|isolate) are random effects that account for variation in growth among replicate plates and repeated growth measurements from the same isolates, respectively.

An initial growth experiment was conducted in May 2018, 2–3 months after the ancestral cultures were challenged to generate resistant cell lines. A follow-up experiment was conducted in September 2019 to observe if COR changed after 15 months of cultivation (~220 generations). A randomized selection of cell lines from each host-virus cross was used in the September 2019 experiment due to resource restraints ($n = 12$). Between growth experiments cell lines were maintained at 25°C, ~100 μE m^{-2} s^{-1}, and passaged approximately every 2 weeks. The September 2019 experiment did not include resistant lines from M1V1 challenges as these lines went extinct in long-term culture. Resistance status was verified in tandem with the second growth experiment by introducing fresh viral lysate to resistant lines and monitoring for a decline in cell density.

RESULTS

Two *Micromonas* isolates from our culture collection, M1 and M2, were chosen for this study, given their susceptibility to the largest number of isolated virus strains in our collection. Virus isolates, referred to here for simplicity as V1, V2, V3, and V4, were chosen to select for resistant *Micromonas* cells. When tested against a suite of seven *Micromonas* isolates in our collection, V1 and V4 had narrower, non-overlapping host ranges, each infecting only 2 of 7 isolates. V2 and V3 had broader, overlapping, but not identical, host ranges, with each infecting 6 of 7 isolates. Prior to selection, M1 was susceptible to infection by V1, V2, and V3, and M2 was susceptible to V2, V3, and V4 (Supplementary Figure S1).

Phylogeny of *Micromonas* and virus isolates

Partial 18S rRNA gene sequences of M1 and M2 revealed 100% nucleotide identity between the two strains. M1 (UHM1061; GenBank accession OQ428650) and M2 (UHM1065; OQ436457), along with another *Micromonas* isolate, UHM1080 (OQ445607), from the oligotrophic Station ALOHA (100 km north of O'ahu, Hawai'i; 22°45′N, 158° W), clustered with members of the species *Micromonas commoda* (Figure 1). Three other published 18S rRNA gene sequences also shared 100% nucleotide identity with M1 and M2, including a sequence from an uncultured eukaryote from the South China Sea (JX188376; Wu et al., 2014) and isolates from pelagic waters in the Sargasso Sea and Pacific Ocean (AY955002; Šlapeta et al., 2006, KU244663; Foulon & Simon, 2016).

The phylogenetic relationships for virus isolates V1, V2, V3, and V4 were more complex than those of the host isolates (Figure 2). The V1 de novo assembly showed evidence of a contaminating sequence. To explore this further, the *polB*-containing contig from V1 was dissolved to obtain component reads, which were then reassembled with stringent settings. This reassembly resulted in two contigs with relatively equal coverage, one with a *polB* gene unique to V1 and another contig with 100% nucleotide identity to the *polB* gene of V4. Thus, V1 may have been contaminated by V4, or the two virus types were co-isolated in the original V1 culture.

The V1 (OQ440138) and V4 (OQ440141) partial *polB* sequences group into a clade with a previously sequenced *Micromonas* virus in our collection, MsV-SA1, isolated from Station ALOHA on *Micromonas* strain UHM1080 (Schvarcz, 2018). This group also contains a *polB* sequence (clone KBvp-16) amplified with phycodnavirus-targeted primers from samples collected from Kāne'ohe Bay (Culley et al., 2009), the location where the viruses used in this study were

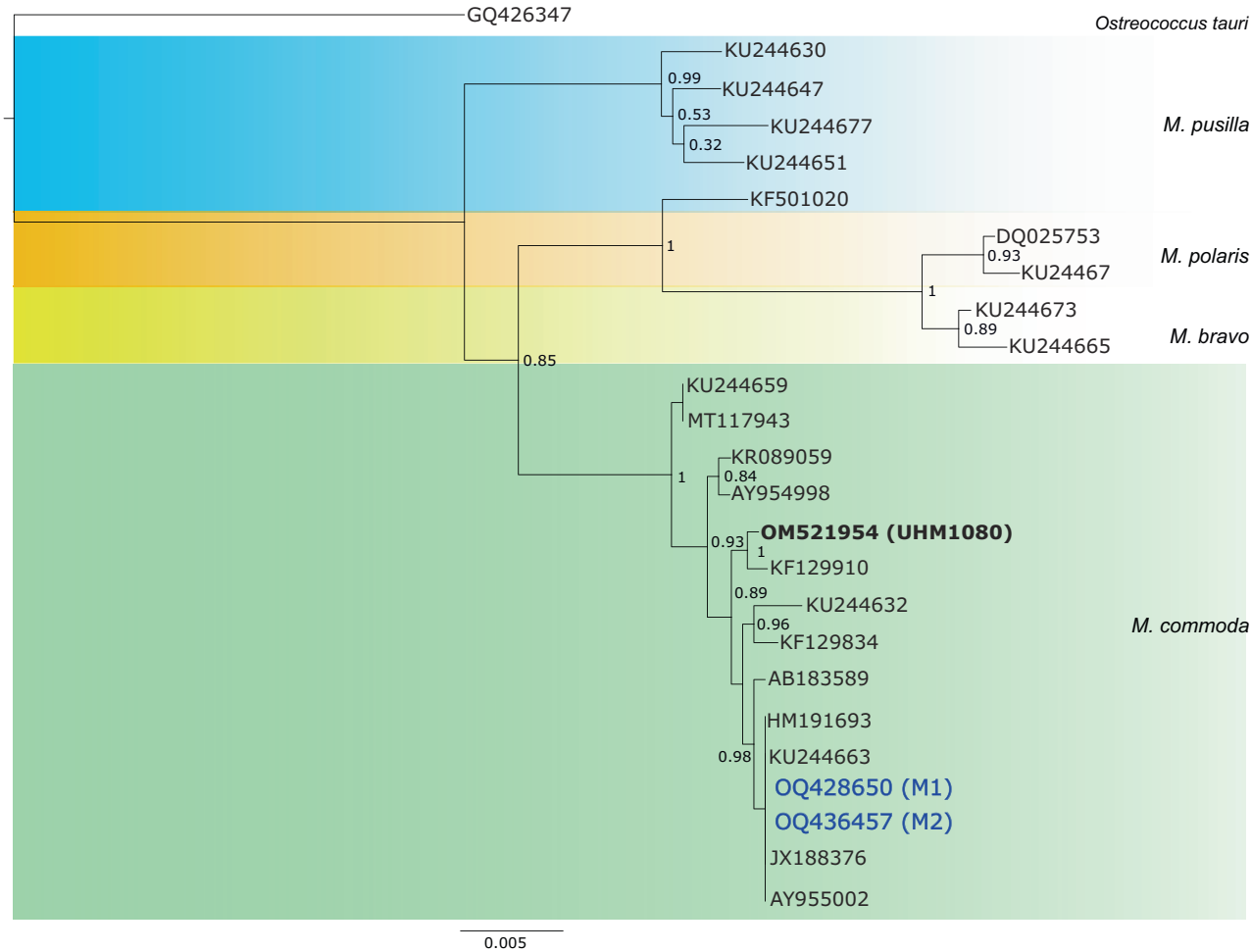

FIGURE 1 Phylogenetic tree of partial 18S rDNA genes of Mamiellales derived from trimmed alignments of 18S rRNA genes from the two *Micromonas* strains used in this study (M1 and M2), a *Micromonas* strain from the pelagic Station ALOHA (UHM1080), and related sequences found using NCBI's BLAST tool. Alignments were created and trimmed with Geneious 11.1 default alignment tool and processed through FastTree using approximately maximum likelihood. Node support values reflect FastTree local support values derived from the Shimodaira–Hasegawa test.

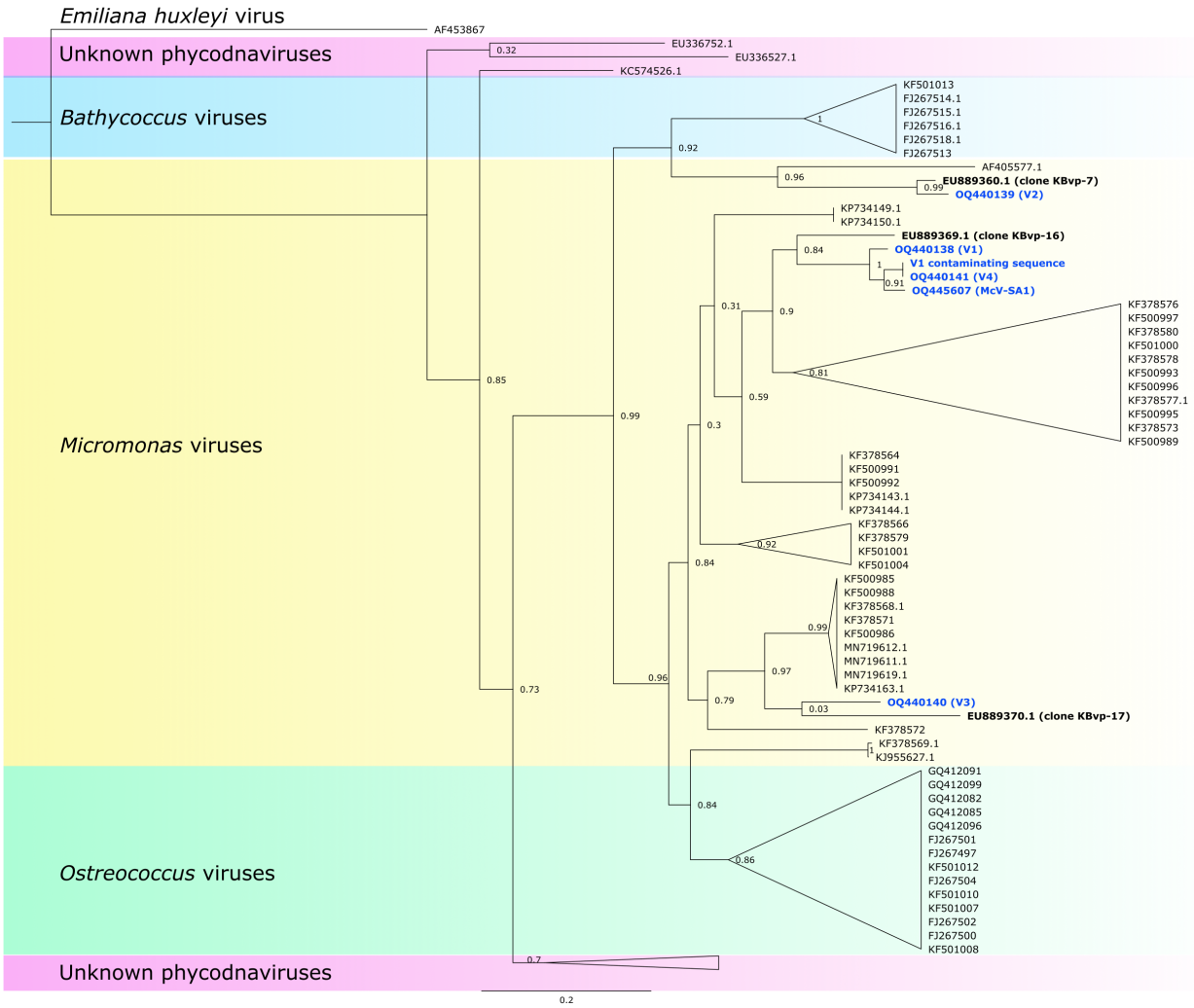

FIGURE 2 Phylogenetic tree of partial polB genes of phycodnaviruses derived from trimmed alignments of *polB* genes of the four viruses used in this study (V1–V4) from coastal waters of Hawai'i, a *Micromonas*-infecting virus isolated on UHM1080 (MsV-SA1) from the open ocean waters off the coast of Hawai'i, and related sequences found through NCBI's BLAST tool. Alignment correction and tree generation were created using the same methodology described in Figure 1.

isolated. V3 (OQ440140) is closely related to another uncultured prasinovirus, KBvp-17, also previously detected in Kāne'ohe Bay (Culley et al., 2009), but these sequences are grouped into a different clade. Finally, V2 (OQ440139) possesses a *polB* sequence that is relatively divergent from other isolated *Micromonas* viruses, with a range of 69.8%–71.3% nucleotide identity with the three other virus strains used in this study. The most closely related sequence to V2 is an uncultured prasinovirus clone, KBvp-7, previously sampled from Kāne'ohe Bay, with 85.7% nucleotide identity (Culley et al., 2009).

Fitness measurements

Our selection experiment yielded 135 cell lines, 88 of which were selected for resistance to infection by one of the viruses, and 47 susceptible lines put through the same dilution-to-extinction process but not exposed to virus (Table 1). Among the 88 resistant cell lines were 11–22 replicates of each cell strain-virus combination. Resulting resistant cell lines were named by concatenating *Micromonas* and virus isolate codes (e.g., there were 11 resistant lines derived from challenging M1 with V1 and these are designated M1V1). Control susceptible cell lines are distinguished from original ancestral strains by appending an 'S' to the original *Micromonas* isolate name (i.e., M1S, M2S). In a study of resistance to viral infection by *Ostreococcus tauri*, Thomas et al. (2011) found continued viral production, perhaps by budding of viruses from intact cells, in a subset of lines that were resistant to lysis. To examine whether viruses were produced by our resistant lines we introduced filtrate from resistant lines to susceptible ancestral cultures, but these showed no

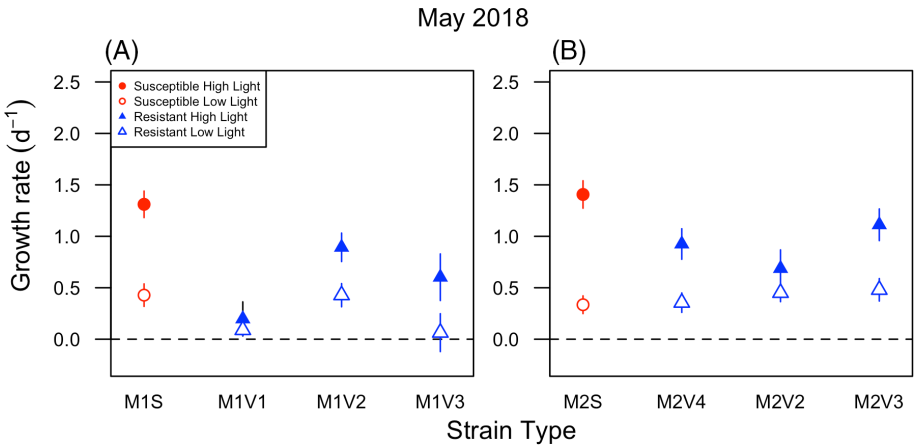

FIGURE 3 Growth rates of susceptible and resistant cell lines in the May 2018 experiment. Panels (A) and (B) show results for M1 and M2, respectively. The plotted points are model-estimated means, averaging over multiple replicate experimental lines ($n = 11$–20; Table 1). Closed circles indicate data from the high light treatment and open circles from the low light treatment. Error bars are 95% confidence intervals. Dotted horizontal lines show 0 days^{-1} growth rate as a reference.

signs of lysis, and therefore we ruled out the possibility that the resistant lines maintained a persistent viral infection.

Growth rates from our initial May 2018 experiment, conducted shortly after isolation of descendant cell lines, showed a significant difference between susceptible and resistant cell lines in high-light conditions (Figure 3; see Supplementary Figures S2 and S3 for raw exponential growth curves). Susceptible M1 lines had a mean growth rate of 1.31 and 0.43 days^{-1} under high light and low light, respectively. Susceptible M2 cells had similar growth rates to M1, at 1.41 and 0.34 days^{-1} under high and low light, respectively. Growth rates of resistant cell lines under high light were consistently lower than their susceptible counterparts (for M1: $p < 0.001$, $\chi^2_1 = 13.2$; for M2: $p < 0.001$, $\chi^2_1 = 9.3$), with the percent decrease in mean growth rates among resistant lines ranging from 21% in M2V3 cells to 85% in M1V1 cells.

Under low light, the effect of resistance on fitness was more variable but significant for both M1 and M2 lines (for M1: $p = 0.01$, $\chi^2_1 = 5.5$; for M2: $p = 0.01$, $\chi^2_1 = 5.9$). However, a positive or negative trend in growth rates among resistant lines was not consistent across all host-virus combinations, with M1 resistant cell lines having slower mean growth rates (0.19 days^{-1}) and M2 resistant cell lines having higher rates (0.43 days^{-1}) than susceptible counterparts (M1: 0.42 days^{-1}, M2: 0.33 days^{-1};Figure 3). Two resistant lines derived from an M1 ancestor grew at slower mean rates (M1V1: 0.09 days^{-1}, M1V3: 0.06 days^{-1}) than susceptible M1S cell lines (0.42 days^{-1}), but one did not (M1V2: 0.43 days^{-1}). The mean growth rate for one set of resistant lines derived from the M2 ancestor (M2V4: 0.36 days^{-1}) was similar to that of the M2S lines (0.33 days^{-1}), but the mean growth rates for two other resistant lines (M2V2: 0.45 days^{-1}, M2V3: 0.48 days^{-1}) were higher than their susceptible counterparts.

Resistant and susceptible cell lines were maintained in culture for approximately 1 year with 1% volume transfer into fresh, virus-free, medium every 2 weeks. M1V1 cell lines went extinct within 6 months of the aforementioned fitness assay. For cell lines that did survive, we re-examined a subset of these (2–3 lines per cross) after 1 year (September 2019), with new lysis assays and growth experiments. We found that all resistant lines had maintained their resistance, despite being propagated in the absence of viruses, and that susceptible lines had maintained their susceptibility. However, new growth patterns had emerged (Figure 4). Mean growth rates of susceptible hosts under high light increased to 1.54 days^{-1} for M1 (previously 1.31 days^{-1}) and 1.83 days^{-1} for M2 (previously 1.41 days^{-1}). An increase in growth rate did not occur at low light for susceptible cell lines. The M1S low light growth rate decreased to 0.37 days^{-1} from 0.42 days^{-1} and M2 maintained its low light growth rate of 0.34 days^{-1}. The strong pattern of decreased fitness of resistant lines under high light seen shortly after selection was not observed 15 months later for host M1 or M2, with no significant differences seen between susceptible and resistant mean growth rates (Figure 4; for M1: $p = 0.74$, $\chi^2_1 = 0.1$; for M2: $p = 0.47$, $\chi^2_1 = 0.5$). When we analysed the highlighted subset on its own, the growth rates of resistant lines (M1V2: 1.56 days^{-1}, M1V3: 1.38 days^{-1}; M2V2: 1.69 days^{-1}, M2V3: 2.05 days^{-1}, M2V4: 1.36 days^{-1}) were the same as, or faster than, their susceptible counterparts on average (M1S: 1.54 days^{-1}; M2S: 1.83 days^{-1}). Only one group of resistant lines (M2V4) maintained a fitness cost similar to that initially seen. Notably, M2V2-derived cell lines had the highest mean growth rate of all lines tested, a 13% higher growth rate than M2 susceptible lines ($p = 0.01$, $\chi^2_1 = 6.2$). Under low light, M1-derived resistant lines did not have mean growth rates different from susceptible counterparts ($p = 0.11$,

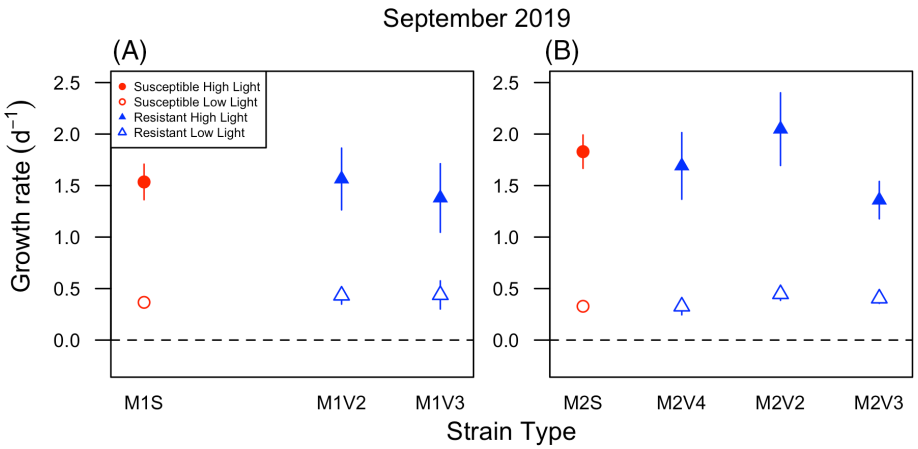

FIGURE 4 Growth rates of susceptible and resistant cell lines in the September 2019 experiment. Panels (A) and (B) show results for M1 and M2, respectively. M1V1 cell lines went extinct before this experiment was conducted. The plotted points are model-estimated means, averaging over multiple replicate experimental lines ($n = 2$–3). Closed circles indicate data from the high light treatment and open circles from the low light treatment. Error bars are 95% confidence intervals. Dotted horizontal lines show 0 days^{-1} growth rate as a reference.

$\chi^2_1 = 2.5$), M2-derived lines did ($p = 0.01$, $\chi^2_1 = 6.5$), with a trend towards increased growth rate.

DISCUSSION

The large number of replicate-resistant lineages (11–20) generated from each host-virus pair improved the power of our statistical analysis, despite variable responses among virus-host pairs. We detected a consistent fitness cost among cell lines that had been selected for resistance to infection 2–3 months prior to growth assays. This fitness cost took the form of lower growth rates under high-light conditions. In contrast, a fitness cost was not consistently present under low light. A subset of resistant cell lines was tested approximately one and a half years later, after verifying continued resistance to population lysis, and the reduction in growth rates under high light disappeared for nearly all observed resistant cell lines. In summary, the presence and magnitude of COR depended on irradiance, identity of host and virus strain, and time since initial selection.

Interplay of resource availability and COR

Our hypothesis, that resource availability would influence the severity of COR, was supported by the results of our May 2018 growth experiments, which showed that the decrease in growth rates for resistant cell lines was larger and more consistent under high light. The mechanism underlying the interaction between light and COR is unknown, but a common mechanism of resistance observed among microbes is the modification or elimination of a cell surface receptor used by the virus for attachment. Viruses in the *Phycodnaviridae* use such receptors to attach to a potential host before inserting their DNA into the cytoplasm (Dunigan et al., 2019). Viral replication then takes place in the nucleus, with virion assembly in the cytoplasm. If the cell surface receptors used for viral attachment are involved in transport of an essential nutrient, their modification via selection for resistance could impair growth rate, as was found in an *Escherichia coli*-phage system (Lenski, 1988). While, Thomas et al. (2011) found evidence that this resistance strategy may not be present in the related protist *Ostreococcus*, this mechanism may still occur in our *Micromonas* cell lines, as any adaptations that result in both viral resistance and a reduction in the maximum uptake rate of a limiting nutrient would be consistent with our observations: Under high light, energy is plentiful so nutrients could be limiting and the cost would be evident, but under low light, energy is limiting and a reduced nutrient uptake rate is of less, or no, consequence. This putative mechanism could be further investigated via viral adsorption assays, in which lower viral adsorption rates would suggest a modification in *Micromonas* cell surface receptors. Measuring nutrient uptake kinetics for susceptible and resistant lines under different light levels would also provide insight into nutrient acquisition by resistant cells, although this approach would be complicated by the slower growth rate of resistant strains, as well as a need to test a multitude of limiting nutrients to determine if one or more are affected.

Greater COR associated with high light may also be explained if light levels at 100 μE m^{-2} s^{-1} cause an unforeseen stress that interacts with an underlying mechanism of resistance. However, our 'high' irradiance of 100 μE m^{-2} s^{-1} is not out of the ordinary for surface waters of Kāne'ohe Bay, the habitat from which these strains were isolated. A study of daily light levels at 2 m depth in the bay over a 14-month period

indicated that photosynthetically active radiation ranged from 0.04 to 1810 μE m^{-2} s^{-1}, with an average daily mean of 85.74 μE m^{-2} s^{-1} (Ritson-Williams & Gates, 2016). Additional experiments using a greater number of light levels would help establish the light level for optimum growth and examine the interplay between light stress and resistance.

Our results differed from some previous work by researchers who studied the interplay between resource availability and viral immunity-associated fitness costs. Heath et al. (2017) tested varying light, phosphate, salinity, and temperature levels for resistant lines of *Ostreococcus tauri*, an alga closely related to *Micromonas*. Heath et al. did not find a correlation between resource level and cost of resistance. One difference among our experiments is the magnitude of resource limitation. Heath et al. compared growth under irradiances of 60 versus 85 μE m^{-2} s^{-1}, which may not shift the factors limiting growth as much as 10 versus 100 μE m^{-2} s^{-1}. It is also possible that the different results in these studies are simply attributable to the differing physiology among species, which may lead to different COR responses.

Fitness costs attenuated over time

Our resistant cultures lost their cost of resistance after 15 months of propagation in the absence of virus, even though they maintained resistance to population lysis. It should be noted that all experimental cultures likely possess some genetic diversity. For example, the ancestral susceptible strains could be used for selection of resistant cells due to the likelihood that rare resistant genotypes were already present in the population. Because the experimentally evolved resistant lines were propagated in the absence of viruses it is possible that genetic diversity increased in these populations during the interim period, and susceptible subpopulations could have been present in the resistant cultures. However, our results indicate that cells with the resistance phenotype continued to dominate the populations because dominance of a susceptible subpopulation would have led to a detectable decline in population density in response to viral inoculation, which was not observed for any of the resistant cell lines. The fact that resistance was maintained, and the resistant population was not outcompeted by a susceptible one, suggests that compensatory mutations occurred that increased growth rate without causing a loss of resistance, as opposed to reversion mutations that would increase growth while also restoring susceptibility to infection. The loss of a fitness cost because of compensatory mutations has been reported in comparable experiments using the prokaryotes *E. coli* (Lenski, 1988) and *Prochlorococcus* (Avrani & Lindell, 2015).

Frickel et al. (2016) conducted a 3-month coevolution experiment with the freshwater green alga *Chlorella variabilis* and its chlorovirus, finding arms race dynamics in which the breadth of host resistance increased over time, while average host growth rate declined over time. These results suggest that continued selective pressure from coevolving viruses may maintain or increase fitness costs, although the results do not rule out growth rate depression being a short-term (i.e., lasting a few months) consequence, comparable to our results. In contrast, researchers using resistant lines that were previously cultured for many years have reported little evidence of depression in growth rates, suggesting that more time allows for the accumulation of compensatory mutations (Heath et al., 2017; Ruiz, Baudoux, et al., 2017; Ruiz, Oosterhof, et al., 2017).

Environmental implications

Based on our observation that COR was greater under high-light conditions, we hypothesize that a higher relative abundance of susceptible cells will occur in natural high-light environments, where the cost to maintain resistance is greater. Given the rapid decline in irradiance with depth in the ocean, depth may play a role in determining the frequency of viral immunity among *Micromonas* populations. In situations where photosynthesis extends below the mixed layer (e.g., shallow mixed layers in relatively clear waters), a comparison of resistance among *Micromonas* populations within the 'high' light mixed layer with 'low' light closer to the base of the euphotic zone, would be worth examining. In addition, if a greater fraction of the population is resistant under lower irradiance, this could mean that a greater fraction of primary production is consumed by zooplankton, rather than being lysed by viruses. Consumption of phytoplankton production by zooplankton transfers energy and nutrients to larger organisms in higher trophic levels, while viral lysis shunts organic matter to the dissolved pool consumed by smaller microbes, and therefore the prevalence of resistance in natural populations may be important for ecosystem size structure and associated differences in carbon export (Wilhelm & Suttle, 1999).

Approaches to measuring fitness costs

Ruiz, Baudoux, et al. (2017) and Ruiz, Oosterhof, et al. (2017) used diverse *Micromonas* and virus isolates from established cultures, rather than experimental evolution, to test for a fitness cost of viral resistance, by asking whether natural variation in the breadth of resistance among the hosts correlated with fitness metrics. The authors did not observe a correlation between

growth rate and the two metrics of resistance used in their study, one metric being defined as the breadth of resistance of a host strain and the other being the viral burst size propagating from a host strain. Those results may be consistent with the findings from our current study, as the lack of a fitness cost in Ruiz, Baudoux, et al. (2017) and Ruiz, Oosterhof, et al. (2017) may reflect compensatory evolution in long-term culture collections after isolation, or in natural populations. It is also possible that a lack of coevolutionary history between the host and virus isolates, or natural variation in host growth rate due to other causes, obscured the effect of resistance.

Our study measured fitness as population growth rate, and it is possible that the temporal dynamics of fitness costs would differ if another measure of fitness was utilized. For example, Thomas et al. (2011) used experimental evolution to study COR in *Ostreococcus tauri* and found no difference in growth rates between resistant and susceptible lines. However, they did find that their resistant cell line declined in direct competition with its susceptible ancestor, which implies that relevant aspects of fitness were not captured by growth rates in batch culture. A follow-up to our work could use competition assays, ideally using interspecific competitors in addition to intraspecific competitors, to see whether competitive differences are maintained over time even as differences in growth rate attenuate.

AUTHOR CONTRIBUTIONS

Anamica Bedi de Silva: Conceptualization; investigation; writing – original draft; methodology; validation; visualization; writing – review and editing; formal analysis; project administration; data curation; software. **Shawn W. Polson:** Conceptualization; investigation; methodology; writing – review and editing; formal analysis; resources; software. **Christopher R. Schvarcz:** Resources; writing – review and editing; investigation. **Grieg F. Steward:** Conceptualization; investigation; methodology; validation; writing – review and editing; funding acquisition; formal analysis; supervision; resources. **Kyle F. Edwards:** Conceptualization; investigation; funding acquisition; methodology; validation; visualization; writing – review and editing; formal analysis; project administration; data curation; supervision; resources; software.

ACKNOWLEDGEMENTS

This work was supported by NSF grants OCE 1559356 and 2129697 (to GFS and KFE) and RII Track-2 FEC 1736030 (to GFS, KFE, and SWP). Special thanks to M. Marston, R. Chong, and K. Selph for comments on previous versions of this manuscript. Thank you to Brewster Kingham and the staff of the University of Delaware Sequencing and Genotyping Center (RRID: SCR_012230) for sequencing our *Micromonas* cell lines. Support from the University of Delaware Bioinformatics Data Science Core Facility (RRID:SCR_017696) including access to additional computational resources was made possible by Delaware INBRE (NIH/NIGMS P20GM103446), the State of Delaware, and the Delaware Biotechnology Institute. Our graphical abstract was created with BioRender.com and published under licence agreement number VX26C3PQRJ.

CONFLICT OF INTEREST STATEMENT

The authors declare no conflict of interest.

DATA AVAILABILITY STATEMENT

The data that support the findings of this study are openly available in Zenodo at https://zenodo.org/doi/10.5281/zenodo.7879605.

ORCID

Anamica Bedi de Silva https://orcid.org/0000-0001-6573-7546
Kyle F. Edwards https://orcid.org/0000-0002-0661-3903

REFERENCES

Altschul, S.F., Gish, W., Miller, W., Meyers, E.W. & Lipman, D.J. (1990) Basic local alignment search tool. *Journal of Molecular Biology*, 3, 403–410.

Avrani, S. & Lindell, D. (2015) Convergent evolution toward an improved growth rate and a reduced resistance range in *Prochlorococcus* strains resistant to phage. *Proceedings of the National Academy of Sciences of the United States of America*, 112, E2191–E2200.

Bellec, L., Grimsley, N., Moreau, H. & Desdevises, Y. (2009) Phylogenetic analysis of new Prasinoviruses (*Phycodnaviridae*) that infect the green unicellular algae *Ostreococcus*, *Bathycoccus* and *Micromonas*. *Environmental Microbiology Reports*, 1, 114–123.

Bohannan, B.J.M., Travisano, M. & Lenski, R.E. (1999) Epistatic interactions can lower the cost of resistance to multiple consumers. *Evolution*, 53, 292.

Breitbart, M. (2012) Marine viruses: truth or dare. *Annual Review of Marine Science*, 4, 425–448.

Brooks, M.L., Fleishman, E., Brown, L.R., Lehman, P.W., Werner, I., Scholz, N. et al. (2012) Life histories, salinity zones, and sublethal contributions of contaminants to pelagic fish declines illustrated with a case study of San Francisco estuary, California, USA. *Estuaries and Coasts*, 35, 603–621.

Chen, F. & Suttle, C.A. (1995) Amplification of DNA polymerase gene fragments from viruses infecting microalgae. *Applied and Environmental Microbiology*, 61, 1274–1278.

Core Team, R. (2022) R: a language and environment for statistical computing.

Cottrell, M. & Suttle, C. (1991) Wide-spread occurrence and clonal variation in viruses which cause lysis of a cosmopolitan, eukaryotic marine phytoplankter Micromonas pusilla. *Marine Ecology Progress Series*, 78, 1–9.

Cottrell, M.T. & Suttle, C.A. (1995) Genetic diversity of algal viruses which lyse the photosynthetic Picoflagellate *Micromonas pusilla* (Prasinophyceae). *Applied and Environmental Microbiology*, 61, 3088–3091.

Culley, A.I., Asuncion, B.F. & Steward, G.F. (2009) Detection of inteins among diverse DNA polymerase genes of uncultivated members of the Phycodnaviridae. *The ISME Journal*, 3, 409–418.

Demory, D., Baudoux, A.-C., Monier, A., Simon, N., Six, C., Ge, P. et al. (2018) Picoeukaryotes of the *Micromonas* genus: sentinels of a warming ocean. *The ISME Journal*, 13, 132–146.

Dunigan, D.D., Al-Sammak, M., Al-Ameeli, Z., Agarkova, I.V., DeLong, J.P. & van Etten, J.L. (2019) Chloroviruses lure hosts through long-distance chemical signaling. *Journal of Virology*, 93, e01688-18.

Edwards, K.F., Thomas, M.K., Klausmeier, C.A. & Litchman, E. (2015) Light and growth in marine phytoplankton: allometric, taxonomic, and environmental variation: light and growth in marine phytoplankton. *Limnology and Oceanography*, 60, 540–552.

Foulon, E. & Simon, N. (2016) *Micromonas commoda* 18S ribosomal RNA gene, partial sequence.

Frada, M.J., Rosenwasser, S., Ben-Dor, S., Shemi, A., Sabanay, H. & Vardi, A. (2017) Morphological switch to a resistant subpopulation in response to viral infection in the bloom-forming coccolithophore *Emiliania huxleyi*. *PLoS Pathogens*, 13, e1006775.

Frickel, J., Sieber, M. & Becks, L. (2016) Eco-evolutionary dynamics in a coevolving host-virus system. *Ecology Letters*, 19, 450–459.

Fuhrman, J.A. (1999) Marine viruses and their biogeochemical and ecological effects. *Nature*, 399, 541–548.

Guillard, R.R.L. (1975) Culture of phytoplankton for feeding marine invertebrates. In: Smith, W.L. & Chanley, M.H. (Eds.) *Culture of marine invertebrate animals*. Boston, MA: Springer US, pp. 29–60.

Guillard, R.R.L. & Ryther, J.H. (1962) Studies of marine planktonic diatoms: I. *Cyclotella nana* Hustedt, and *Detonula confervacea* (Cleve) Gran. *Canadian Journal of Microbiology*, 8, 229–239.

Heath, S., Knox, K., Vale, P. & Collins, S. (2017) Virus resistance is not costly in a marine alga evolving under multiple environmental stressors. *Viruses*, 9, 39.

Koren, S., Walenz, B.P., Berlin, K., Miller, J.R., Bergman, N.H. & Phillippy, A.M. (2017) Canu: scalable and accurate long-read assembly via adaptive *k*-mer weighting and repeat separation. *Genome Research*, 27, 722–736.

Lennon, J.T., Khatana, S.A.M., Marston, M.F. & Martiny, J.B.H. (2007) Is there a cost of virus resistance in marine cyanobacteria? *The ISME Journal*, 1, 300–312.

Lenski, R.E. (1988) Experimental studies of pleiotropy and epistasis in *Escherichia coli*. II. Compensation for Maldaptive effects associated with resistance to virus T4. *Evolution*, 42, 433.

Price, M.N., Dehal, P.S. & Arkin, A.P. (2010) FastTree 2–approximately maximum-likelihood trees for large alignments. *PLoS One*, 5, e9490.

Ritson-Williams, R. & Gates, R.D. (2016) Kaneohe Bay light data 2014 and 2015.

Ruiz, E., Baudoux, A.-C., Simon, N., Sandaa, R.-A., Thingstad, T.F. & Pagarete, A. (2017) *Micromonas* versus virus: new experimental insights challenge viral impact: *Micromonas*—MicV empirical estimations. *Environmental Microbiology*, 19, 2068–2076.

Ruiz, E., Oosterhof, M., Sandaa, R.-A., Larsen, A. & Pagarete, A. (2017) Emerging interaction patterns in the *Emiliania huxleyi*-EhV system. *Viruses*, 9, 61.

Sayers, E.W., Bolton, E.E., Brister, J.R., Canese, K., Chan, J., Comeau, D.C. et al. (2022) Database resources of the national center for biotechnology information. *Nucleic Acids Research*, 50, D20–D26.

Schvarcz, C.R. (2018) Cultivation and characterization of viruses infecting eukaryotic phytoplankton from the tropical North Pacific Ocean.

Schwartz, D.A. & Lindell, D. (2017) Genetic hurdles limit the arms race between *Prochlorococcus* and the T7-like podoviruses infecting them. *The ISME Journal*, 11, 1836–1851.

Šlapeta, J., López-García, P. & Moreira, D. (2006) Global dispersal and ancient cryptic species in the smallest marine eukaryotes. *Molecular Biology and Evolution*, 23, 23–29.

Suttle, C.A. (2007) Marine viruses—major players in the global ecosystem. *Nature Reviews. Microbiology*, 5, 801–812.

Thomas, R., Grimsley, N., Escande, M., Subirana, L., Derelle, E. & Moreau, H. (2011) Acquisition and maintenance of resistance to viruses in eukaryotic phytoplankton populations. *Environmental Microbiology*, 13, 1412–1420.

Thomsen, H.A. & Buck, K.R. (1998) Nanoflagellates of the central California waters: taxonomy, biogeography and abundance of primitive, green flagellates (Pedinophyceae, Prasinophyceae). *Deep Sea Research Part II: Topical Studies in Oceanography*, 45, 1687–1707.

Thyrhaug, R., Larsen, A., Thingstad, T. & Bratbak, G. (2003) Stable coexistence in marine algal host-virus systems. *Marine Ecology Progress Series*, 254, 27–35.

Våge, S., Storesund, J.E. & Thingstad, T.F. (2013) Adding a cost of resistance description extends the ability of virus-host model to explain observed patterns in structure and function of pelagic microbial communities: structuring of microbial communities by viruses. *Environmental Microbiology*, 15, 1842–1852.

Waterbury, J.B. & Valois, F.W. (1993) Resistance to co-occurring phages enables marine *Synechococcus* communities to coexist with cyanophages abundant in seawater. *Applied and Environmental Microbiology*, 59, 3393–3399.

Waters, R.E. & Chan, A.T. (1983) *Micromonas pusilla* virus: the virus growth cycle and associated physiological events within the host cells; host range mutation. *The Journal of General Virology*, 63, 199–206.

Wilhelm, S.W. & Suttle, C.A. (1999) Viruses and nutrient cycles in the sea—viruses play critical roles in the structure and function of aquatic food webs. *Bioscience*, 49, 8.

Wilson, W.H., van Etten, J.L. & Allen, M.J. (2009) The Phycodnaviridae: the story of how tiny giants rule the world. In: van Etten, J. L. (Ed.) *Lesser known large dsDNA viruses*. *Current topics in microbiology and immunology*. Berlin, Heidelberg: Springer, pp. 1–42.

Wu, W., Huang, B. & Zhong, C. (2014) Photosynthetic picoeukaryote assemblages in the South China Sea from the Pearl River estuary to the SEATS station. *Aquatic Microbial Ecology*, 71, 271–284.

Zingone, A. (1999) Seasonal dynamics in the abundance of *Micromonas pusilla* (Prasinophyceae) and its viruses in the Gulf of Naples (Mediterranean Sea). *Journal of Plankton Research*, 21, 2143–2159.

SUPPORTING INFORMATION

Additional supporting information can be found online in the Supporting Information section at the end of this article.

How to cite this article: Bedi de Silva, A., Polson, S.W., Schvarcz, C.R., Steward, G.F. & Edwards, K.F. (2024) Transient, context-dependent fitness costs accompanying viral resistance in isolates of the marine microalga *Micromonas* sp. (class Mamiellophyceae). *Environmental Microbiology*, 26(8), e16686. Available from: https://doi.org/10.1111/1462-2920.16686